In Vitro Dimerization of the Bovine Papillomavirus E5 Protein Transmembrane Domain[†]

Joanne Oates,[‡] Matthew Hicks,[‡] Timothy R. Dafforn,[§] Daniel DiMaio,[||] and Ann M. Dixon*[,‡]

Department of Chemistry, University of Warwick, Coventry CV4 7AL, United Kingdom, Department of Biological Sciences, University of Birmingham, Birmingham B15 2TT, United Kingdom, and Departments of Genetics, Therapeutic Radiology, and Molecular Biophysics and Biochemistry, Yale University School of Medicine, New Haven, Connecticut 06510

Received April 9, 2008; Revised Manuscript Received June 17, 2008

ABSTRACT: The E5 protein from bovine papillomavirus is a type II membrane protein and the product of the smallest known oncogene. E5 causes cell transformation by binding and activating the platelet-derived growth factor beta receptor (PDGFβR). In order to productively interact with the receptor, it is thought that E5 binds as a dimer. However, wild-type E5 and various mutants have also been shown to form trimers, tetramers, and even higher order oligomers. The residues in E5 that drive and stabilize a dimeric state are also still in question. At present, two different models for the E5 dimer exist in the literature, one symmetric and one asymmetric. There is universal agreement, however, that the transmembrane (TM) domain plays a vital role in stabilizing the functional oligomer; indeed, mutation of various TM domain residues can abolish E5 function. In order to better resolve the role of the E5 TM domain in function, we have undertaken the first quantitative *in vitro* characterization of the E5 TM domain in detergent micelles and liposomes. Circular and linear dichroism analyses verify that the TM domain adopts a stable α-helical structure and is able to partition efficiently across lipid bilayers. SDS−PAGE and analytical ultracentrifugation demonstrate for the first time that the TM domain of E5 forms a strong dimer with a standard state free energy of dissociation of 5.0 kcal mol^{-1}. We have used our new results to interpret existing models of E5 dimer formation and provide a direct link between TM helix interactions and E5 function.

Tumor viruses "transform" healthy cells into cancerous cells by encoding what are known as viral transforming proteins in their genome. A primary function of these proteins is to activate cellular growth pathways, and they can do this by either mimicking cell receptors or by activating native receptors (*1, 2*). A well-known viral transforming protein is the E5 protein from bovine papillomavirus (BPV).[1] E5 transforms cells by binding to the platelet-derived growth factor beta receptor (PDGFβR) (*3*), a receptor tyrosine kinase. E5 binding results in receptor dimerization, transphosphorylation, and sustained activation (*4, 5*), leading to uncontrolled cell growth.

E5 is the smallest known viral transforming protein containing only 44 amino acids (Figure 1a), with a highly hydrophobic central domain which partitions into the cell membrane (*6, 7*). Investigations carried out *in vivo* suggest that E5 must undergo homodimerization in order to efficiently activate PDGFβR. *In vivo* data also suggest that the E5 dimer interacts uniquely with the transmembrane (TM) domain of PDGFβR (*8–10*), in contrast to its native ligand (PDGF) which binds in the large extracellular domain of the receptor. This interaction is an excellent example of TM domains as contributors to specific protein−protein interactions (*11–16*).

In vivo mutagenesis of E5 and PDGFβR has led to identification of several amino acids in the TM domains of both proteins that are critical for complex formation and activation (*9, 17–21*). These results have given rise to the current model for the E5/PDGFβR complex (Figure 1b), stabilized by hydrogen bonding and electrostatic interactions of residues in both proteins (*22*). Mutagenesis has also suggested a critical role for disulfide bond-forming cysteine residues at the C-terminus of E5. The transforming activity of E5 can be blocked by mutagenesis of these cysteines and then restored by addition of a heterologous dimerization domain (*17, 21, 23*).

Despite extensive study of this protein, there is still a lack of consensus as to the molecular organization of E5 and the driving force for oligomer formation. Thus far, *in vivo* mutagenesis (*17, 20, 21*), Fourier transform infrared spectroscopy (FTIR) (*22*), and molecular dynamics simulation (*22, 24*) have been applied to the study of full-length E5. From these studies, two different models have emerged for E5, a symmetric dimer and an asymmetric dimer. The most recent model describes a symmetric dimer (Figure 1c), where

[†] This work was supported by Cancer Research UK (CR-UK) Grant C21449/A6926 to A.M.D. and by NIH Grant CA37157 to D.D.

* To whom correspondence should be addressed. Tel: 0 (44) 24761 50037. Fax: 9 (44) 24765 24112. E-mail: ann.dixon@warwick.ac.uk.

[‡] University of Warwick.

[§] University of Birmingham.

[||] Yale University School of Medicine.

[1] Abbreviations: AUC, analytical ultracentrifugation; BPV, bovine papillomavirus; CD, circular dichroism; DOF, degrees of freedom; DMPC, 1,2-dimyristoyl-*sn*-glycero-3-phosphocholine; DPC, dodecylphosphocholine; FTIR, Fourier transfrorm infrared spectroscopy; LD, linear dichroism; MRE, mean residue elipticity; PDGF, platelet-derived growth factor; RMSD, root-mean-square deviation; SDS−PAGE, sodium dodecyl sulfate−polyacrylamide gel electrophoresis; SRS, sum of residuals squared; SRV, square root of variance; TFA, trifluoroacetic acid; TFE, 2,2,2-trifluoroethanol; TM, transmembrane.

10.1021/bi8006252 CCC: $40.75
Published on Web 08/02/2008

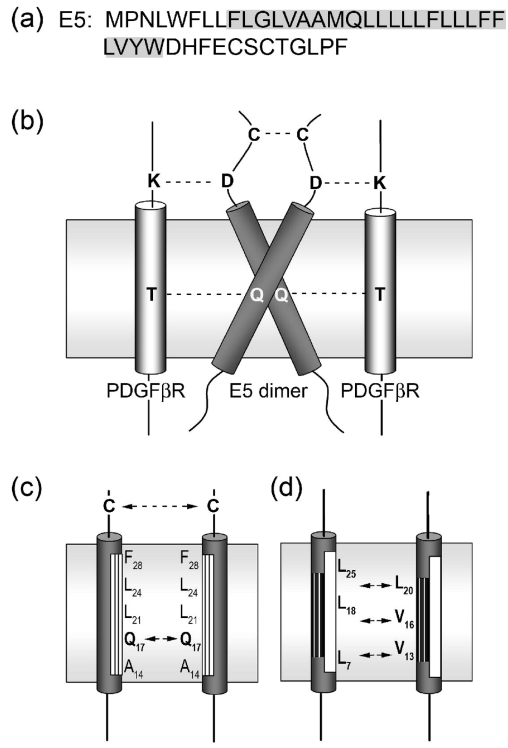

FIGURE 1: (a) Sequence of full-length BPV E5 protein. The predicted transmembrane domain is highlighted (shaded box). (b) The current model of the E5/PDGFβ receptor complex, showing the interaction of a disulfide-bonded E5 homodimer with the transmembrane domain of the receptor. Mutagenesis suggests that this complex is stabilized by electrostatic interactions between D_{33} of E5 and K_{499} of the receptor as well as hydrogen bonding between Q_{17} of E5 and T_{513} of the receptor. (c) Current model of the E5 homodimer, as shown in panel b. The symmetrical dimer is stabilized by C-terminal disulfide bonds and interhelical hydrogen bonding of Q_{17} and contains residues A_{14}, Q_{17}, L_{21}, L_{24}, and F_{28} at the dimer interface. (d) The asymmetric model of the E5 dimer, stabilized by the packing of L_7, L_{18}, and L_{25} on one monomer against V_{13}, V_{16}, and L_{20} of another monomer.

E5 TM domain residues A_{14}, Q_{17}, L_{21}, L_{24}, and F_{28} are proposed to lie at the dimer interface (*21, 22, 24*). The dimer is thought to be partially stabilized by interactions within the TM domain, specifically by an interchain hydrogen bond between the membrane-embedded Q_{17} residues of two monomers, a feature consistent with findings that apolar point mutations at position 17 impair E5 dimer formation *in vivo* (*23, 25*). In addition, this model also suggests that the C-terminal cysteine residues play a major role in E5 dimerization via disulfide bond formation (Figure 1b). An alternative, asymmetric model for the E5 dimer has also been proposed in the literature (*20*). This model describes the packing of two different "faces" of the predicted TM helix, where a face composed of L_7, L_{18}, and L_{25} is thought to pack against a face containing V_{13}, V_{16}, and L_{20} (Figure 1d), and the authors suggest that *functional* dimers are formed via a series of stepwise rearrangements to obtain the lowest energy and optimum conformation needed to interact with PDGFβR (*20*).

All of the studies described above imply a central role for the TM domain of E5 in functional dimer assembly, but there is little direct experimental evidence to support this. We have previously shown that the E5 TM domain in isolation strongly oligomerizes using the TOXCAT assay (*24*), an assay in which TM domain interactions are assayed within a natural bilayer environment. However, this assay does not report on oligomeric state. In fact, the conclusion that the native state of the E5 protein is a dimer and not a higher order oligomer rests largely on the mobility of the native protein during SDS−PAGE under nonreducing conditions. Using this method, E5 has also been shown to form trimers, tetramers, and even higher order oligomers (*20*).

To better resolve the oligomeric state of E5 and the role of the TM domain in function, we present here the first quantitative biophysical evidence that the E5 TM domain forms stable dimers that can insert across membrane bilayers. We use a number of complementary biophysical techniques to report on the secondary structure, bilayer orientation, stoichiometry, and binding energy of the TM domain. The results support existing models of E5 dimers, confirm the ability of the E5 TM domain to independently drive dimerization, and highlight the critical role of this domain in function.

EXPERIMENTAL PROCEDURES

Peptide Sequence and Purification. A peptide corresponding to the TM domain of E5 ($E5_{TM}$) was synthesized by the Keck Facility at Yale University using F-moc chemistry. The sequence of the $E5_{TM}$ peptide was KKKFLGLVAAMQLLLLLFLLLFFLVYWDHK, containing residues F_9−H_{34} from E5 as well as non-native lysine residues to aid solubility and end caps on the C- and N- termini. The peptide was purified by reversed-phase HPLC using a linear acetonitrile gradient including 0.1% trifluoroacetic acid (TFA) on a Phenomenex C4 column. The purity of pooled fractions was confirmed by mass spectrometry before subsequent lyophilization.

Circular Dichroism (CD). CD experiments were carried out using a Jasco J715 spectropolarimeter (Jasco UK, Great Dunmow, U.K.) and 1 mm path-length quartz cuvettes (Starna; Optiglass Ltd., Hainault, U.K.), equipped with a Peltier thermally controlled cuvette holder. Spectra were recorded between 190 and 260 nm with a data pitch of 0.2 nm, a bandwidth of 2 nm, a scanning speed of 100 nm min^{-1}, and a response time of 1 s. The $E5_{TM}$ peptide was prepared in 50 mM sodium phosphate buffer (pH 7.5), containing 15 mM dodecylphosphocholine (DPC) (Avanti Polar Lipids, Alabaster, AL) and 100 mM NaCl, to a final peptide concentration of 114 μM. CD spectra were collected at 10 °C intervals between 5 and 95 °C. Data shown were averaged from four individual spectra and were truncated at 200 nm below which absorbance was too high to give reliable data. Measurement of the buffer without peptide was subtracted to obtain the final spectra.

Liposome Preparation. Liposomes containing $E5_{TM}$ peptide were prepared by codissolving lipid (1,2-dimyristoyl-*sn*-glycero-3-phosphocholine (DMPC)) (Avanti Polar Lipids, Alabaster, AL) and peptide in 2,2,2-trifluoroethanol (TFE), at a ratio of 10:1 lipid to peptide. The mixture was dried under nitrogen and placed under vacuum overnight to ensure complete removal of the organic phase. The resulting lipid−-peptide film was reconstituted in 50 mM sodium phosphate buffer, pH 7, and subjected to five freeze−thaw cycles using an ethanol/dry ice bath and a water bath set at 40 °C, followed by sonication at 40 °C for 5 min.

Linear Dichroism (LD). LD spectra were measured at room temperature between 190 and 400 nm. Acquisition parameters (bandwidth, etc.) were identical to those described for CD measurements. Samples were aligned in a microvolume Couette cell (*26, 27*) using applied voltages of 3, 4, and 5 V (corresponding to rotation speeds of 3K, 4K, and 5K rpm, respectively). Data shown are an average of 16 individual scans and are truncated at 210 nm where absorbance was too high to give reliable data. Spectra of the nonaligned sample (i.e., with no rotation) were subtracted from the aligned data and smoothed (using the binomial smoothing function in Jasco spectra analysis program, version 1.53.01 [build 1]) to obtain the final spectra. The Couette cell used was built in-house; equivalent models are commercially available (Kromatek, Great Dunmow, U.K.).

SDS−Polyacrylamide Gel Electrophoresis (SDS−PAGE). SDS−PAGE was carried out using NuPAGE 12% Bis-tris gels (Invitrogen, Paisley, U.K.). Typically, samples were prepared in 50 mM sodium phosphate buffer (pH 7.5), containing 10 mM SDS and 100 mM NaCl. Peptide concentrations were estimated from the absorbance at 280 nm using a molar extinction coefficient (ϵ_{280}) of 6990 mol^{-1} cm^{-1} for $E5_{TM}$. Peptide visualization was achieved by staining either with Coomassie-R250 or with silver nitrate.

Analytical Ultracentrifugation. Sedimentation equilibrium and sedimentation velocity measurements were carried out on a Beckman XL-I/A analytical ultracentrifuge (Beckman Coulter, Fullerton, CA). $E5_{TM}$ peptide samples were prepared in 50 mM sodium phosphate buffer (pH 7.5), containing 15 mM DPC (Avanti Polar Lipids, Alabaster, AL), 100 mM NaCl, and 52.5% D_2O (Cambridge Isotope Laboratories, Andover, MA) to match the buoyant density of the detergent. When the solvent matches the buoyant density of the detergent micelles, the only contribution to the buoyant molecular weight is from the peptide, as described (*28*). Data were collected at 25 °C using absorbance optics set to 280 nm. For sedimentation equilibrium a six-channel centerpiece was used. Measurements were taken at three peptide concentrations (29, 72, and 114 μM) and three speeds (37000, 40000, and 43000 rpm). Samples were centrifuged for time periods in excess of those required to reach equilibrium (20 h per speed), and establishment of sedimentation equilibrium was verified using the program WinMatch to subtract successive scans until no difference was observed. The $E5_{TM}$ peptide monomeric molecular mass and partial specific volume in 52.5% D_2O were determined to be 3685 Da (corrected for H−D exchange) and 0.8059 mL g^{-1}, respectively, using the program SEDNTERP (available at http://www.rasmb.bbri.org/). Global fitting of the nine data sets was undertaken by nonlinear least squares curve fitting using Win-NONLIN (*29*). Assuming that the contribution of any bound detergent is negated by the addition of D_2O, the data were fit to eq 1:

$$c_{\text{total}} = c_{\text{monomer},r_0} e^{(\omega^2/2RT)M(1-\bar{\nu}\rho)(r^2-r_0^2)} + c_{n\text{-mer},r_0} e^{[(\omega^2/2RT)nM(1-\bar{\nu}\rho)(r^2-r_0^2)]} \quad (1)$$

where c_{total} is the total absorbance at a radial position; c_{monomer} is the monomer absorbance at a reference position, r_0; M is the monomer molecular mass; $\bar{\nu}$ is the monomer partial specific volume; ρ is the solvent density (calculated as 1.059 g mL^{-1} as reported previously (*30*)); ω is the angular velocity (radians per second); R is the universal gas constant; T is the absolute temperature; and $c_{n\text{-mer}}$ is the n-mer absorbance at a reference position, r_0. The value of n is chosen by the operator to represent the stoichiometry required for fitting. Goodness of fit was determined by examination of the spread of the residuals around the best fit and minimization of variance. As a single global association constant could be used to describe the data, the reaction was shown to be reversible on the time scale of the experiment. The molar association constant for a monomer−dimer equilibrium (k_{1-2}) was calculated according to eq 2, assuming that the extinction coefficient of the n-mer is n times that of the monomer:

$$k_{1-2_{\text{conc}}} = k_{1-2_{\text{abs}}} \varepsilon l/2 \quad (2)$$

where $k_{1-2\text{abs}}$ is the association constant in absorbance units, ϵ is the molar extinction coefficient, and l is the path length. The apparent free energy of dissociation (ΔG_{app}) and the mole fraction standard state free energy of dissociation (ΔG°_x, which accounts for detergent concentration) were calculated according to eqs 3 and 4, respectively (*31*):

$$\Delta G_{\text{app}} = -RT \ln K_{\text{app}} \quad (3)$$

$$\Delta G^\circ_x = \Delta G_{\text{app}} - RT \ln [\text{micellarDet}]_w \quad (4)$$

where K_{app} is the apparent dissociation constant ($1/k_{1-2,\text{conc}}$) obtained from the fit and $[\text{micellarDet}]_w$ is the concentration of detergent in the micellar phase.

Sedimentation velocity data were collected at a peptide concentration of 114 μM using a double-channel centerpiece and a speed of 40000 rpm. A total of 400 scans were recorded in each case, with 50 s between each scan. Fitting of the resulting profiles was achieved using SEDFIT (*32*) to generate a continuous sedimentation coefficient distribution, which was subsequently converted to a molecular mass distribution. The buffer density was the same as that used for the equilibrium experiment, and the buffer viscosity was calculated as 1.01026 cP using SEDNTERP.

RESULTS

The E5 TM Domain Forms a Thermally Stable α*-Helix in DPC Micelles.* To investigate TM domain interactions of the E5 protein *in vitro*, we synthesized a peptide corresponding to the E5 TM domain ($E5_{TM}$, residues F_9−H_{34}). Lysine residues were added at the N- and C-termini to aid solubility of this highly hydrophobic peptide and reduce nonspecific aggregation. This approach has been shown in a number of studies not to affect the properties of strongly interacting TM domain peptides (*33–35*). However, for more weakly interacting TM helices, there are examples in the literature in which lysine and other positively charged residues abolish dimerization, and they should therefore be used with caution (*36, 37*).

The full-length E5 protein has been shown to be predominantly α-helical in synthetic membrane bilayers using FTIR (*22*). To determine the secondary structure of the $E5_{TM}$ peptide in detergent micelles, CD spectra were acquired for peptide reconstituted into the zwitterionic detergent dodecylphosphocholine (DPC). The resulting spectra (Figure 2) show a characteristic α-helical profile, with negative absorption maxima at 208 and 222 nm, demonstrating that the $E5_{TM}$

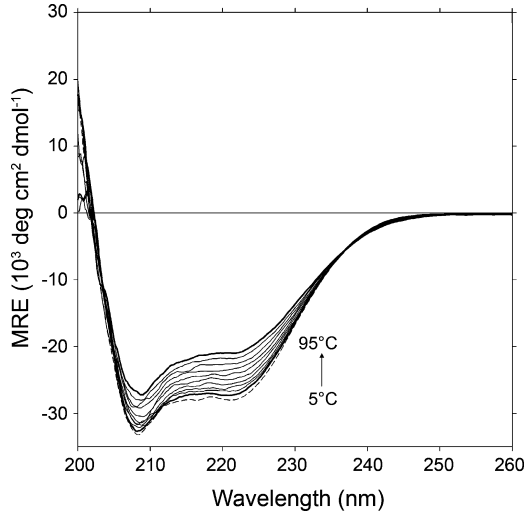

FIGURE 2: Circular dichroism spectra of purified $E5_{TM}$ synthetic peptide solubilized in buffer containing 15 mM DPC. Individual spectra (solid lines) were collected while increasing the temperature from 5 to 95 °C in 10 °C increments using a Peltier thermally controlled cuvette holder. Reversibility of melting was confirmed by cycling the temperature back to 5 °C and remeasuring the spectrum (dashed line). Data are reported in units of mean residue elipticity (MRE).

peptide is α-helical in DPC micelles. Fitting of CD data collected at 25 °C using K2d software (*38*) indicates that the peptide is approximately 88% α-helical. This helical secondary structure is very stable over a large temperature range. Only a small decrease in α-helical structure was observed between 5 and 95 °C, and the process was completely reversible (see dotted line in Figure 2), a phenomenon that has been observed previously for other detergent-solubilized TM peptides (*39*).

$E5_{TM}$ Peptide Inserts into Lipid Vesicles. FTIR was also used to demonstrate that the full-length E5 protein inserts into synthetic lipid bilayers *in vitro* (*22*). To investigate whether the α-helical $E5_{TM}$ peptide retains the ability of the full-length protein to effectively partition into lipid bilayers (*22*), we have employed the solution-phase method of linear dichroism spectroscopy (LD) (*40, 41*). Recent technical advances in LD have enabled the use of small sample volumes (<50 μL) (*26, 27*), facilitating its application to study of membrane proteins (*41*). The signal obtained in LD results from the difference in absorption of horizontally and vertically polarized light by a sample aligned parallel to one of the polarization axes (usually the horizontal direction). Therefore, samples for LD must be capable of being aligned, which means that the molecules under investigation must be asymmetric in either charge or shape. Liposomes are well suited to this technique as they can be flow-aligned in a rapidly spinning Couette cell to produce elongated shapes (Figure 3a) (*41, 42*). If there is no interaction between peptide and liposomes, the peptide will not align, and therefore no difference in the absorption of the two polarizations of light (LD signal) will be observed (Figure 3a). If the peptide inserts as an α-helix across the bilayer (i.e., orients perpendicular to the membrane), a broad positive LD signal centered at approximately 230 nm (absorbance maximum for peptide bond) will be observed, whereas peptides lying on the surface of the membrane (i.e., oriented parallel to the bilayer) will yield a negative LD signal at this wavelength (*40, 41*).

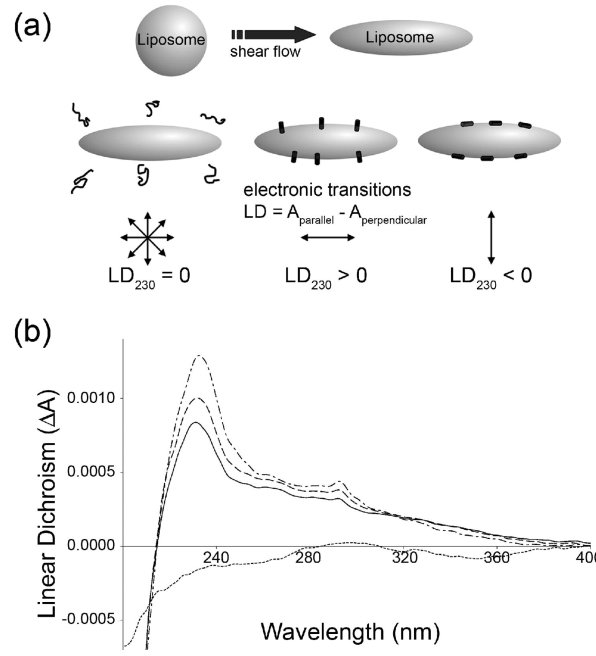

FIGURE 3: (a) Linear dichroism of peptides in liposomes relies on the alignment of liposomes by shear flow, with the parallel direction defined as the flow direction (top row). Peptides are too small to align by themselves and only give an LD signal when associated with the aligned liposomes (middle row). Different orientations of peptide will result in different average directions for transition moments of the peptide. For example the n to π^* transition of the peptide bond in an α-helix (around 230 nm) is oriented perpendicular to the helix axis and will give rise to the LD signals indicated in the bottom part of the diagram. Note that the lower energy π to π^* transition of the peptide bond in an α-helix (around 210 nm) should give the opposite sign signal. (b) Linear dichroism spectra of $E5_{TM}$ peptide in micelles and in liposomes: $E5_{TM}$ peptide in DPC micelles rotating at 5000 rpm (dotted line) and $E5_{TM}$ peptide in liposomes rotating at 5000 rpm (dash-dotted line), 4000 rpm (dashed line), and 3000 rpm (solid line).

We investigated the interaction between the $E5_{TM}$ peptide and synthetic lipid bilayers by acquiring LD spectra of the peptide in flow-aligned DMPC liposomes and, as a control, in DPC micelles. The LD spectrum of DMPC liposomes was also recorded, and no absorption in the wavelength range of interest was observed (data not shown). Figure 3b shows the resulting LD spectra collected at different rotation speeds for the $E5_{TM}$ peptide in DMPC bilayers. In all three spectra, we observe a large, positive absorption peak centered at 230 nm, demonstrating that the $E5_{TM}$ peptide is preferentially inserted across the membrane bilayer. The positive gradient across the spectra for the liposome-containing samples is due to an increase in light scattering with decreasing wavelength. The increase in peptide LD signal intensity with increasing rotation speed is due to the increase in alignment of the liposomes, demonstrating that the LD signal of the peptide is dependent on alignment as expected for a peptide inserted across the bilayer. The small positive peak at ~290 nm results from absorbance of the tryptophan side chain, indicating that this side chain is ordered in the peptide−membrane complex. As expected, there is negligible LD signal in the micelle sample (Figure 3b) as micelles are too small to align.

The E5 TM Domain Forms Stable Homodimers. In order to determine the oligomeric state of the E5 TM domain, SDS−PAGE was used to analyze $E5_{TM}$ peptide samples over a range of concentrations (3−173 μM). As shown in Figure

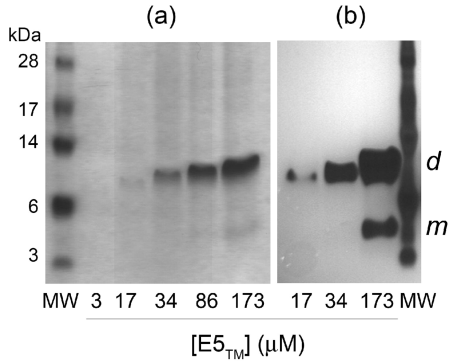

FIGURE 4: SDS−PAGE results for purified $E5_{TM}$ peptide run alongside molecular mass standards (MW). (a) Analysis of the $E5_{TM}$ peptide was carried out over a range of concentrations (stated below each lane) and yielded primarily dimers (dimer MW = 7.32 kDa), labeled *d* in the Coomassie stained gel, with only a trace of monomer (*m*) visible at the highest concentrations. (b) The presence of $E5_{TM}$ monomers was more clearly revealed by silver staining.

4a, Coomassie blue was only able to detect the $E5_{TM}$ peptide at concentrations above 17 μM. Above this concentration, the peptide predominantly runs as a single discrete band with a molecular mass of approximately 10 kDa. Only at the highest concentration of total peptide (173 μM) is a second weak band visible at approximately 5 kDa.

This very weak band becomes more easily visible upon silver staining (Figure 4b), a method that is well-known to be 100−1000 times more sensitive than staining with Coomassie blue. It is difficult to isolate the exact source of this enhanced sensitivity, as the binding mechanisms involved in silver staining still remain unclear (*43*). However, studies thus far suggest that silver ions coordinate to the protein via high-affinity binding sites known to be very active in metal binding, such as amino, imidazole, and sulfydryl groups on amino acid side chains (*44*). In contrast, Coomassie blue dye binds to basic and aromatic amino acids via noncovalent interactions, the affinities of which depend heavily on the identity of the amino acid and the protocol used (*45*). Perhaps most importantly in the analysis of membrane proteins, Coomassie binding is sensitive to interference from detergents (*46*).

The positions of the $E5_{TM}$ peptide bands at 5 and 10 kDa on the SDS−PAGE gel do not correspond exactly with the monomer and dimer molecular masses predicted from the sequence (3.66 and 7.32 kDa, respectively). Similar aberrant behavior on SDS−PAGE gels has been documented for other membrane proteins and is thought to stem from conformational effects (*47*), making data interpretation difficult. Nevertheless, the two bands in the SDS−PAGE gel of the $E5_{TM}$ peptide were thought to correspond to monomer (at 5 kDa) and dimer (at 10 kDa). The fact that we see two distinct bands in the gel also suggests that exchange between the two states is slow relative to the time scale of the experiment, and the association is reversible (*13*).

The SDS−PAGE results suggest that a monomer−dimer equilibrium exists for the E5 TM domain but that this equilibrium is heavily weighted toward formation of dimers. The formation of SDS-stable dimers is not well-understood, but we do know that the chemical properties of detergents play a key role in the lateral association of TM helices (*48*). In many cases, SDS is unable to completely denature these transmembrane peptides; indeed, experiments have shown

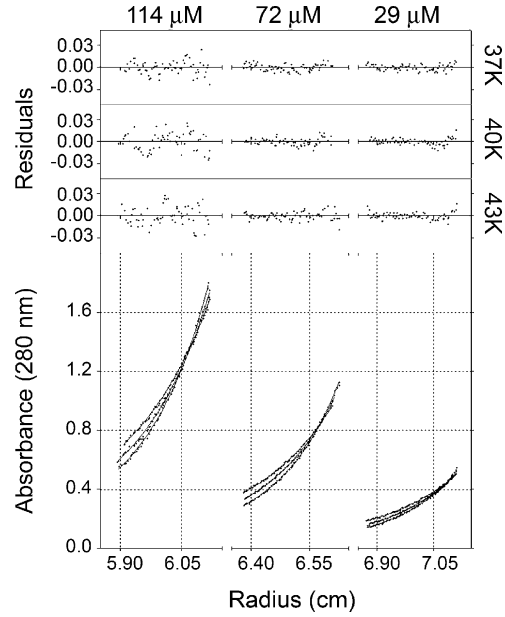

FIGURE 5: Sedimentation equilibrium data obtained for $E5_{TM}$ peptide in buffer containing 15 mM DPC and 52.5% D_2O. Shown in the lower three plots are the data collected at three concentrations, ranging from 114 to 29 μM. At each concentration, data were collected at three speeds (37000, 40000, and 43000 rpm). Dots represent experimental data, and solid curves display the best fit resulting from global analysis of all nine data sets, in this case the fit of a model representing a monomer−dimer equilibrium. Above each plot are the residuals of the fitting process.

that SDS is able to induce formation of helical secondary structure during membrane protein refolding (*49–51*). Additionally, positively charged residues in the peptide (K, R, H) can interact with the negatively charged headgroup of SDS, and depending on the position of the residue in the sequence, these interactions could potentially have either a stabilizing or destabilizing effect (*37*).

In order to more quantitatively determine the oligomeric state of the TM domain and derive thermodynamic parameters for the interaction, the $E5_{TM}$ peptide was analyzed by analytical ultracentrifugation (AUC). AUC is a technique that is rapidly gaining recognition as a powerful tool in the study of membrane protein assembly and interactions. Both sedimentation equilibrium and sedimentation velocity experiments were employed in this study, as they yield complementary information about the size and shape of proteins. Sedimentation equilibrium analyses were carried out at three speeds and three peptide concentrations in DPC detergent micelles, and the concentration versus radial distance profiles for each set of conditions are shown in Figure 5. The data were initially fit to a monomer model, followed by fitting to models of increasing complexity as described (*52, 53*). The model of best fit is identified when the square root of variance (SRV) of the fit is minimized and the residuals of the fit are distributed randomly about zero. The statistics from each fit are summarized in Table 1, showing that a minimum value for the SRV was obtained when the data were fit to either a monomer−dimer model or a monomer−dimer−tetramer model. Both of these models also resulted in the most random fit residuals. The monomer−dimer model was further supported by fitting of the data to a single species model, which yielded a molecular mass close to that of dimer. In all models tested, inclusion of a nonideality factor was required in the

Table 1: Nonlinear Least Squares Fitting Statistics[a] for Sedimentation Equilibrium Data and Resulting Dissociation Constants[b] for the E5 TM Domain

			K_d (M)	
fit	SRV ($\times 10^{-3}$)	DOF	dimer	tetramer
M	223	586		
M/D	7.60	584	4.4×10^{-6}	
M/Tr	8.58	584		
M/Tet	9.72	584		
M/D/Tet	7.63	584	4.1×10^{-6}	3.0×10^{-10}

[a] Statistics are given for fits to monomer (M), monomer−dimer (M/D), monomer−trimer (M/Tr), monomer−tetramer (M/Tet), and monomer−dimer−tetramer (M/D/Tet) equilibria. Variance of fit, sum of residuals squared (SRS), square root of variance (SRV), and the number of degrees of freedom in the fit (DOF) are shown. [b] Also shown are the apparent dissociation constants (K_d) as calculated from the fits for both dimer and tetramer.

analysis to obtain a good fit to the data. Inclusion of a nonideality parameter was justified in this case as a decrease in the weight-average molecular mass was observed with increasing concentration. Nonideal behavior of an associating system can result from charge or crowding effects and is incorporated into the model using the second virial coefficient, *B*. In the case of protein detergent complexes, nonideality most likely results from the detergent itself (*54*) or from electrostatic interactions (*55*).

The results of the sedimentation equilibrium experiments allowed us to narrow down the possible oligomeric states of the E5 TM domain. In order to select from the two best-fit models, sedimentation velocity analyses were also conducted using identical buffer conditions. Sedimentation velocity can be difficult with peptides of low molecular mass due to the high speeds necessary to minimize the rate of back diffusion; however, a speed of 40000 rpm was sufficient to produce data with the required mass resolution. Fitting residuals and sedimentation profiles are shown in panels a and b of Figure 6, respectively, with the fit data corresponding to an RMSD of 9.75×10^{-3}. The resulting sedimentation coefficient profile contains a single species centered at $S = 0.275$ (Figure 6c), corresponding to a molecular mass for the $E5_{TM}$ peptide of 7.27 kDa (which agrees to within 1% of the calculated molecular mass of the dimer, 7.32 kDa). This fit produced a frictional ratio of 2.54, suggesting a significantly elongated ellipsoidal shape for the E5 TM domain dimer, as would be expected for rod-shaped TM α-helices.

Because the sedimentation velocity analyses clearly indicated that $E5_{TM}$ was predominantly a dimer, we used the monomer−dimer model to determine dissociation constants from the sedimentation equilibrium data. Residuals from global fitting of the data to a single monomer−dimer dissociation constant are shown in Figure 5. Analysis of the dimer fit yielded an apparent monomer−dimer dissociation constant ($K_{d,app}$) of 4 μM in 15 mM DPC and a corresponding apparent free energy of dissociation $\Delta G_{app} = 7.4$ kcal mol^{-1} at 25 °C. To facilitate comparison of this value to other published data and take into account the detergent concentration (which can significantly effect the measured energetics of TM dimerization), ΔG_{app} was then converted to a mole fraction standard state free energy of dissociation as described in eq 4 and in ref *31*. This conversion resulted in a free energy of dissociation of 5.0 kcal mol^{-1} for the E5 TM dimer (as compared to 7.0 kcal mol^{-1} for GpA (*31*)).

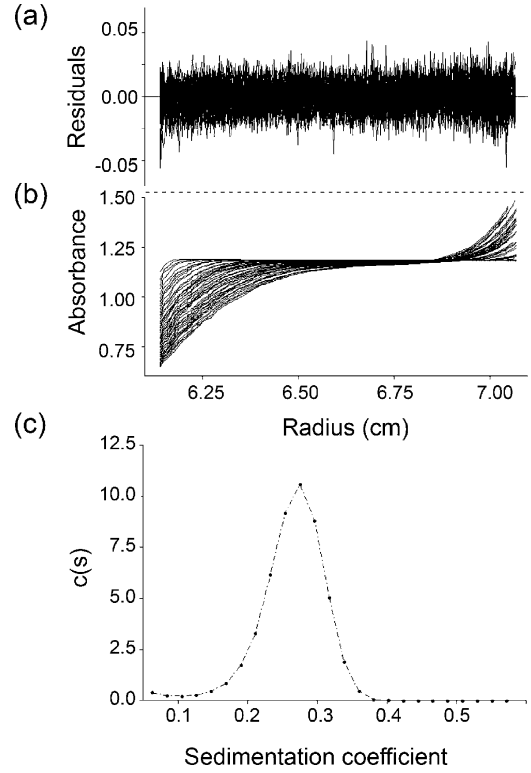

FIGURE 6: Sedimentation velocity data obtained for $E5_{TM}$ peptide in buffer containing 15 mM DPC and 52.5% D_2O. (a) Residuals of the fitting process. (b) Raw data showing the sedimentation profiles of the peptide over the time course of the experiment. (c) Sedimentation coefficient distribution profile as calculated using the SEDFIT program. Conversion of sedimentation coefficients to molecular mass yielded a peak value of 7.27 kDa, which agrees closely to the theoretical mass for the dimer (7.32 kDa).

In combination, the *in vitro* data from SDS−PAGE and AUC clearly demonstrate for the first time that the E5 TM domain forms a strong dimer in both SDS and DPC detergent micelles, providing strong evidence for the central role of the TM domain in E5 homodimer formation and function.

DISCUSSION

In vivo studies of E5 have implicated the TM domain in dimerization and function, but its precise role in this process remained unclear (*20–22, 24*). We have previously reported that the TM domain of E5 strongly self-associates in natural membranes using the TOXCAT assay (*24*). Furthermore, we found that the self-association of the TM domain was highly dependent on a centrally located glutamine residue (Q_{17}), a property that has also been observed in the full-length protein (*25*). However, TOXCAT can only provide a relative measure of affinity (relative to GpA) and does not provide a quantitative measure of either the oligomeric state or the thermodynamic properties of the process.

Here, we report the first investigation of the E5 TM domain *in vitro*. This approach has allowed us to directly determine the oligomeric state of the E5 TM and thus its contribution to formation of a functional E5 oligomer. We have observed experimentally the ability of the α-helical E5 TM domain to insert into lipid bilayers approximately parallel to the membrane normal using Couette flow linear dichroism spectroscopy. We have also observed the ability of the TM domain to form SDS-stable homodimers, properties it shares with the full-length protein *in vivo* and *in vitro* (*6, 22*).

Furthermore, analytical ultracentrifugation has provided the first thermodynamic description of E5 TM dimerization in DPC detergent micelles. We report a free energy of dissociation (ΔG_d) of 5.0 kcal mol^{-1}, which is comparable to other strongly dimerizing TM domains (i.e., GpA) (*52*). These data allow us to say with some confidence that the information encoded within the E5 TM domain is sufficient to drive insertion and dimerization of the protein within biological membranes, a conclusion implied in previous studies (*20, 21*) but not demonstrated experimentally until now. It is likely that C-terminal disulfide bonds in E5 contribute to stability of the dimer *in vivo* but probably do not define the structure.

In focusing our attention specifically on the TM domain, we have begun to unravel the mechanism of E5 function by providing a quantitative description of the TM-driven dimerization process. The ability of the TM domain to form strong dimers ($K_{d,app} = 4\ \mu M$) has significant implications for future structural studies of E5, which would be greatly simplified by removal of the cysteine residues. Understanding the precise requirements for E5 dimerization is essential in unraveling the molecular details that govern the interaction of this protein with PDGFβR and ultimately its ability to transform cells. Furthermore, study of the critical role of TM domain interactions in this system may also shed new light on the fundamental principles which govern TM-mediated interactions between membrane proteins.

ACKNOWLEDGMENT

We thank J. Crawford for peptide synthesis, Professor A. Rodger for helpful discussions, critical reading of the manuscript, and the use of the circular and linear dichroism spectrophotometers, and Professor T. D. H. Bugg for critical reading of the manuscript.

REFERENCES

1. Drummond-Barbosa, D., and DiMaio, D. (1997) Virocrine transformation. *Biochim. Biophys. Acta 1332*, M1–M17.
2. DiMaio, D., Lai, C. C., and Klein, O. (1998) Virocrine transformation: the intersection between viral transforming proteins and cellular signal transduction pathways. *Annu. Rev. Microbiol. 52*, 397–421.
3. DiMaio, D., Lai, C. C., and Mattoon, D. (2000) The platelet-derived growth factor beta receptor as a target of the bovine papillomavirus E5 protein. *Cytokine Growth Factor Rev. 11*, 283–293.
4. Lai, C. C., Henningson, C., and DiMaio, D. (1998) Bovine papillomavirus E5 protein induces oligomerization and transphosphorylation of the platelet-derived growth factor beta receptor. *Proc. Natl. Acad. Sci. U.S.A. 95*, 15241–15246.
5. Petti, L., and DiMaio, D. (1992) Stable association between the bovine papillomavirus E5 transforming protein and activated platelet-derived growth factor receptor in transformed mouse cells. *Proc. Natl. Acad. Sci. U.S.A. 89*, 6736–6740.
6. Burkhardt, A., DiMaio, D., and Schlegel, R. (1987) Genetic and biochemical definition of the bovine papillomavirus E5 transforming protein. *EMBO J. 6*, 2381–2385.
7. Schlegel, R., Wade-Glass, M., Rabson, M. S., and Yang, Y. C. (1986) The E5 transforming gene of bovine papillomavirus encodes a small hydrophobic protein. *Science 233*, 464–467.
8. Goldstein, D. J., Li, W., Wang, L. M., Heidaran, M. A., Aaronson, S., Shinn, R., Schlegel, R., and Pierce, J. H. (1994) The bovine papillomavirus type 1 E5 transforming protein specifically binds and activates the beta-type receptor for the platelet-derived growth factor but not other related tyrosine kinase-containing receptors to induce cellular transformation. *J. Virol. 68*, 4432–4441.
9. Nappi, V. M., Schaefer, J. A., and Petti, L. M. (2002) Molecular examination of the transmembrane requirements of the platelet-derived growth factor beta receptor for a productive interaction with the bovine papillomavirus E5 oncoprotein. *J. Biol. Chem. 277*, 47149–47159.
10. Petti, L. M., Reddy, V., Smith, S. O., and DiMaio, D. (1997) Identification of amino acids in the transmembrane and juxtamembrane domains of the platelet-derived growth factor receptor required for productive interaction with the bovine papillomavirus E5 protein. *J. Virol. 71*, 7318–7327.
11. Booth, P. J. (2000) Unravelling the folding of bacteriorhodopsin. *Biochim. Biophys. Acta 1460*, 4–14.
12. Huang, K. S., Bayley, H., Liao, M. J., London, E., and Khorana, H. G. (1981) Refolding of an integral membrane protein. Denaturation, renaturation, and reconstitution of intact bacteriorhodopsin and two proteolytic fragments. *J. Biol. Chem. 256*, 3802–3809.
13. Lemmon, M. A., Flanagan, J. M., Hunt, J. F., Adair, B. D., Bormann, B.-J., Dempsey, C. E., and Engelman, D. M. (1992) Glycophorin A dimerization is driven by specific interactions between transmembrane α-helices. *J. Biol. Chem. 267*, 7683–7689.
14. Lemmon, M. A., Flanagan, J. M., Treutlein, H. R., Zhang, J., and Engelman, D. M. (1992) Sequence specificity in the dimerization of transmembrane alpha-helices. *Biochemistry 31*, 12719–12725.
15. Popot, J. L., and Engelman, D. M. (1990) Membrane protein folding and oligomerization: the two-stage model. *Biochemistry 29*, 4031–4037.
16. Popot, J. L., and Engelman, D. M. (2000) Helical membrane protein folding, stability and evolution. *Annu. Rev. Biochem. 69*, 881–922.
17. Horwitz, B. H., Burkhardt, A., Schlegel, R., and DiMaio, D. (1988) 44-amino acid E5 transforming protein of bovine papillomavirus requires a hydrophobic core and specific carboxyl-terminal amino acids. *Mol. Cell. Biol. 8*, 4071–4078.
18. Nilson, L. A., Gottlieb, R. L., Polack, G. W., and DiMaio, D. (1995) Mutational analysis of the interaction between the bovine papillomavirus E5 transforming protein and the endogenous beta receptor for platelet-derived growth factor in mouse C127 cells. *J. Virol. 69*, 5869–5874.
19. Klein, O., Kegler-Ebo, D., Su, J., Smith, S., and DiMaio, D. (1999) The bovine papillomavirus E5 protein requires a juxtamembrane negative charge for activation of the platelet-derived growth factor beta receptor and transformation of C127 cells. *J. Virol. 73*, 3264–3272.
20. Adduci, A. J., and Schlegel, R. (1999) The transmembrane domain of the E5 oncoprotein contains functionally discrete helical faces. *J. Biol. Chem. 274*, 10249–10258.
21. Mattoon, D., Gupta, K., Doyon, J., Loll, P. J., and DiMaio, D. (2001) Identification of the transmembrane dimer interface of the bovine papillomavirus E5 protein. *Oncogene 20*, 3824–3834.
22. Surti, T., Klein, O., Aschheim, K., DiMaio, D., and Smith, S. O. (1998) Structural models of the bovine papillomavirus E5 protein. *Proteins 33*, 601–612.
23. Meyer, A. N., Xu, Y. F., Webster, M. K., Smith, A. E., and Donoghue, D. J. (1994) Cellular transformation by a transmembrane peptide: structural requirements for the bovine papillomavirus E5 oncoprotein. *Proc. Natl. Acad. Sci. U.S.A. 91*, 4634–4638.
24. Freeman-Cook, L. L., Dixon, A. M., Frank, J. B., Xia, Y., Ely, L., Gerstein, M., Engelman, D. M., and DiMaio, D. (2004) Selection and characterization of small random transmembrane proteins that bind and activate the platelet-derived growth factor beta receptor. *J. Mol. Biol. 338*, 907–920.
25. Klein, O., Polack, G. W., Surti, T., Kegler-Ebo, D., Smith, S. O., and DiMaio, D. (1998) Role of glutamine 17 of the bovine papillomavirus E5 protein in platelet-derived growth factor beta receptor activation and cell transformation. *J. Virol. 72*, 8921–8932.
26. Marrington, R., Dafforn, T. R., Halsall, D. J., MacDonald, J. I., Hicks, M., and Rodger, A. (2005) Validation of new microvolume Couette flow linear dichroism cells. *Analyst 130*, 1608–1616.
27. Marrington, R., Dafforn, T. R., Halsall, D. J., and Rodger, A. (2004) Micro-volume couette flow sample orientation for absorbance and fluorescence linear dichroism. *Biophys. J. 87*, 2002–2012.
28. Kochendoerfer, G. G., Salom, D., Lear, J. D., Wilk-Orescan, R., Kent, S. B., and DeGrado, W. F. (1999) Total chemical synthesis of the integral membrane protein influenza A virus M2: role of its C-terminal domain in tetramer assembly. *Biochemistry 38*, 11905–11913.
29. Johnson, M. L., Correia, J. J., Yphantis, D. A., and Halvorson, H. R. (1981) Analysis of data from the analytical ultracentrifuge by nonlinear least-squares techniques. *Biophys. J. 36*, 575–588.
30. Salom, D., Hill, B. R., Lear, J. D., and DeGrado, W. F. (2000) pH-dependent tetramerization and amantadine binding of the

transmembrane helix of M2 from the influenza A virus. *Biochemistry 39*, 14160–14170.
31. Fleming, K. G. (2002) Standardizing the free energy change of transmembrane helix-helix interactions. *J. Mol. Biol. 323*, 563–571.
32. Schuck, P. (2000) Size distribution analysis of macromolecules by sedimentation velocity ultracentrifugation and Lamm equation modelling. *Biophys. J. 78*, 1606–1619.
33. Melnyk, R. A., Partridge, A. W., Yip, J., Wu, Y., Goto, N. K., and Deber, C. M. (2003) Polar residue tagging of transmembrane peptides. *Biopolymers 71*, 675–685.
34. Ding, F. X., Xie, H., Arshava, B., Becker, J. M., and Naider, F. (2001) ATR-FTIR study of the structure and orientation of transmembrane domains of the *Saccharomyces cerevisiae* alpha-mating factor receptor in phospholipids. *Biochemistry 40*, 8945–8954.
35. Lazarova, T., Brewin, K. A., Stoeber, K., and Robinson, C. R. (2004) Characterization of peptides corresponding to the seven transmembrane domains of human adenosine A2a receptor. *Biochemistry 43*, 12945–12954.
36. Iwamoto, T., You, M., Li, E., Spangler, J., Tomich, J. M., and Hristova, K. (2005) Synthesis and initial characterization of FGFR3 transmembrane domain: consequences of sequence modifications. *Biochim. Biophys. Acta 1668*, 240–247.
37. Prodohl, A., Weber, M., Dreher, C., and Schneider, D. (2007) A mutational study of transmembrane helix-helix interactions. *Biochimie 89*, 1433–1437.
38. Merelo, J. J., Andrade, M. A., Prieto, A., and Morán, F. (1994) Proteinotopic feature maps. *Neurocomputing* 443–454.
39. Zhou, F. X., Cocco, M. J., Russ, W. P., Brunger, A. T., and Engelman, D. M. (2000) Interhelical hydrogen bonding drives strong interactions in membrane proteins. *Nat. Struct. Biol. 7*, 154–160.
40. Dafforn, T. R., and Rodger, A. (2004) Linear dichroism of biomolecules: which way is up? *Curr. Opin. Struct. Biol. 14*, 541–546.
41. Rodger, A., Rajendra, J., Marrington, R., Ardhammar, M., Norden, B., Hirst, J. D., Gilbert, A. T. B., Dafforn, T. R., Halsall, D. J., Woolhead, C. A., Robinson, C., Pinheiro, T. J. T., Kazlauskaite, J., Seymour, M., Perez, N., and Hannon, M. J. (2002) Flow oriented linear dichroism to probe protein orientation in membrane environments. *Phys. Chem. Chem. Phys. 4*, 4051–4057.
42. Ardhammar, M., Mikati, N., and Norden, B. (1998) Chromophore Orientation in Liposome Membranes Probed with Flow Dichroism. *J. Am. Chem. Soc. 120*, 9957–9958.
43. Rabilloud, T. (1990) Mechanisms of protein silver staining in polyacrylamide gels: a 10-year synthesis. *Electrophoresis 11*, 785–794.
44. Merril, C. R., and Pratt, M. E. (1986) A silver stain for the rapid quantitative detection of proteins or nucleic acids on membranes or thin layer plates. *Anal. Biochem. 156*, 96–110.
45. Georgiou, C. D., Grintzalis, K., Zervoudakis, G., and Papapostolou, I. (2008) Mechanism of Coomassie brilliant blue G250 binding to proteins: A hydrophobic assay for nanogram quantities of proteins. *Anal. Bioanal. Chem. 391*, 391–403.
46. Bradford, M. M. (1976) A rapid and sensitive method for the quantitation of microgram quantities of protein utilizing the principle of protein-dye binding. *Anal. Biochem. 72*, 248–254.
47. Therien, A. G., Grant, F. E. M., and Deber, C. M. (2001) Interhelical hydrogen bonds in the CFTR membrane domain. *Nat. Struct. Mol. Biol. 8*, 597–601.
48. Fisher, L. E., Engelman, D. M., and Sturgis, J. N. (2003) Effect of detergents on the association of the glycophorin A transmembrane helix. *Biophys. J. 85*, 3097–3105.
49. Booth, P. J. (2003) The trials and tribulations of membrane protein folding in vitro. *Biochim. Biophys. Acta 1610*, 51–56.
50. Braiman, M. S., Stern, L. J., Chao, B. H., and Khorana, H. G. (1987) Structure-function studies on bacteriorhodopsin. IV. Purification and renaturation of bacterio-opsin polypeptide expressed in *Escherichia coli*. *J. Biol. Chem. 262*, 9271–9276.
51. Plumley, F. G., and Schmidt, G. W. (1987) Reconstitution of chlorophyll a/b light-harvesting complexes: Xanthophyll-dependent assembly and energy transfer. *Proc. Natl. Acad. Sci. U.S.A. 84*, 146–150.
52. Fleming, K. G., Ackerman, A. L., and Engelman, D. M. (1997) The effect of point mutations on the free energy of transmembrane α helix dimerization. *J. Mol. Biol. 272*, 266–275.
53. Dixon, A. M., Stanley, B. J., Matthews, E. E., Dawson, J. P., and Engelman, D. M. (2006) Invariant chain transmembrane domain trimerization: a step in MHC class II assembly. *Biochemistry 45*, 5228–5234.
54. Hitscherich, C., Jr., Kaplan, J., Allaman, M., Wiencek, J., and Loll, P. J. (2000) Static light scattering studies of OmpF porin: implications for integral membrane protein crystallization. *Protein Sci. 9*, 1559–1566.
55. Holladay, L. A., and Sohpianolpoulos, A. J. (1972) Nonideal associating systems. I. Documentation of a new method for determining the parameters from sedimentation equilibrium data. *J. Biol. Chem. 247*, 427–439.

BI8006252